Femto-to-Femto (F2F) Communication: The Next Evolution Step in 5G Wireless Backhauling

Anup Chaudhari and C. Siva Ram Murthy
Department of Computer Science and Engineering
Indian Institute of Technology Madras, Chennai 600036, India
anup.chaudhari93@gmail.com, murthy@iitm.ac.in

***Abstract*—The future 5G cellular networks are expected to support several-fold increase in data traffic and number of devices, and provide a very low latency and gigabit-rate data services. millimeter Wave (mmWave) communication (30 – 300 GHz) is proposed to be an important part of the 5G cellular networks to fulfill these requirements. With most of the high data rate demands originating from indoor User Equipments (UEs), conventional wired backhaul links prove to be a major bottleneck. Hence, mmWave wireless backhaul links are explored at Femto Base Stations (FBSs). In order to derive maximum benefit of mmWave backhaul links, efficient resource (data slots) utilization is necessary. Proper scheduling of mmWave backhaul links will help to achieve the same. In this paper, we propose a novel FBS-to-FBS (F2F) communication scheme which not only helps in offloading the data traffic from the Micro Base Station (MiBS) but also can act as a relay link for the other FBSs for routing the backhaul traffic to the MiBS. We also propose a solution to concurrently schedule mmWave wireless backhaul links to increase the resource utilization considering the coexistence of both FBS-to-MiBS (F2M) and F2F links. Our proposed solution consists of two parts – first, it determines which backhaul links can be scheduled concurrently by finding the upper bound for the interfering distance based on the alignment of different lobes of the directional antennas. Second, the transmit power is throttled to match the Quality of Service (QoS) requirements of each link aiming to further control the interference and to increase the number of concurrent transmissions. The benefits of the proposed solution are studied and compared with the Time Division Multiple Access (TDMA) and random scheduling schemes using extensive simulations.**

***Index Terms*—mmWave, 5G cellular network, FBS-to-FBS (F2F) communication, backhaul link scheduling, QoS, power control**

I. Introduction

Cellular broadband users are increasingly using data-intensive applications such as high definition video streaming, ultra fast file transfer, augmented reality, and virtual reality games which result in multi-gigabit data rate requirement [1]. However, most of these requests are generated by indoor User Equipments (UEs) associated with low powered Femto Base Stations (FBSs) [2]. Hence, in order to satisfy these data rate requirements the radio access (FBS-UE) link capacity is increased with the help of higher cellular spectrum reuse, unlicensed carrier aggregation using Licensed Assisted Access (LAA), and millimeter Wave (mmWave) techniques. However, most of the techniques in the literature have ignored the fact that the current Digital Subscriber Line (DSL) and Asymmetric Digital Subscriber Line (ADSL) based FBS backhaul links do not offer the required data rate. This prevents FBSs from utilizing their full radio access link capacity. Optical fiber links have the necessary capacity to fulfil the FBS backhaul requirements. However, their high deployment and maintenance costs are preventing them from being widely used. The backhaul problem is further complicated with the prediction that the number of FBSs are going to increase exponentially in the near future [3]. Thus, mmWave links between 30 GHz and 300 GHz are being utilized to satisfy the backhaul rate requirements of future 5G cellular networks [4], [5], [6], [7]. mmWave wireless backhaul links between FBSs and Micro Base Stations (MiBSs) not only fulfil the data rate requirements but are also flexible and cost effective as compared to wired backhaul links. However, due to high free space path loss, considerable oxygen absorption, sensitivity to blockages by obstacles such as walls, humans, and furnitures both MiBSs and FBSs are expected to be equipped with a highly directional antenna in future 5G cellular networks to achieve higher data rate and larger transmission range.

Existing research on mmWave transmission and link scheduling is mostly focused on Wireless Personal Area Network (WPAN) and Wireless Local Area Network (WLAN) [8], [9], [10]. The authors in [8] have introduced the concept of exclusive region to allow concurrent transmissions by exploiting spatial reuse for WPAN. In [9] vertex multiple coloring concurrent transmission scheme for Device-to-Device (D2D) network over 60 GHz spectrum is proposed. The scheme proposed in [9] gives preference to the flows having better prospects for higher data rate. The authors in [10] have explored spatial-time division multiple-access scheduling algorithm for mmWave based WPAN by concurrently scheduling both interfering and non-interfering links to transmit while fulfilling the Quality of Service (QoS) requirements of each link. In [11] the authors have addressed a resource sharing scheme by allowing non-interfering D2D links to operate concurrently in a mmWave 5G cellular network.

To the best of our knowledge, we are the first to demonstrate the benefits of using FBS-to-FBS (F2F) communication in 5G mmWave cellular networks. F2F communication provides a direct link between two FBSs without any intervention of the MiBS. This not only helps in offloading the data traffic from the MiBS (for e.g., UE-FBS-FBS-UE instead of UE-MiBS-UE) but also can act as a relay link for the other FBSs for routing the backhaul traffic to the MiBS. Such a communication can be highly beneficial in forwarding the high volume of data

978-3-901882-90-6/17 ©2017 IFIP

generated by autonomous vehicles in typical mmWave based Vehicular Ad-Hoc Networks (VANETs) supported by FBSs. Another application is carrying aggregated traffic generated by Internet of Things (IOT) devices, where FBS can act as a gateway and can transfer data to other FBSs present in the proximity. F2F communication, with the availability of directional antennas, also helps in increasing the system capacity by exploiting the spatial reuse. In order to maximize the resource utilization, we thus study a concurrent backhaul [FBS-to-MiBS (F2M) and F2F] link scheduling scheme with transmit power control based on QoS requirements.

The rest of the paper is organized as follows. We explain system model in Section II for mmWave communication in cellular networks. Section III discusses the optimization problem to schedule backhaul links. Then, we discuss our proposed solution in Section IV by defining interference range constraint, determining interference graph and performing QoS based power control. Section V presents the performance evaluation and obtained results. The work is concluded in Section VI along with some future research directions.

II. System Model

Our network model consists of a two-dimensional (2D) dense deployment of F FBSs within the coverage area of an MiBS of radius R. The coverage area of the MiBS is divided into S $(= \frac{2\pi}{\theta'})$ sectors, where θ' is the beamwidth of a directional antenna serving the FBSs located in a sector. Any two antennas of the MiBS can either transmit or receive simultaneously without interfering with each other. In our system both FBSs and MiBS employ electronically steerable directional antenna for data transmission and reception. Similar to D2D communication we exploit direct communication between two FBSs (F2F) without any intervention of the MiBS. F2F communication not only helps in offloading the traffic from the MiBS but also increases the system capacity by exploiting the spatial reuse of directional links. Our system consists of two types of links – F2M (uplink) and F2F. We consider Time Division Duplexing (TDD) while scheduling different links. We analyze the uplink system behavior only. In order to avoid interference two interfering links are scheduled in two different data slots but multiple non-interfering links can be scheduled simultaneously within a single data slot. In order to maximize the probability of Line-of-Sight (LOS) between MiBS and FBS, the mmWave backhaul transceiver is kept at the roof top and is wired to the indoor FBS.

A. Antenna Model

In order to overcome the very high path loss because of extremely high frequency and other atmospheric attenuation higher gain directional antenna at both transmitter and receiver is used for mmWave communication. Transmitter and receiver can direct their beams toward each other by using electronically steerable antenna arrays in order to achieve maximum transmission rate. An antenna array consists of numerous antenna elements and uses beam forming techniques to direct its beam in the required direction [12]. The size of an antenna element is very small for mmWave communication, hence it is feasible to incorporate numerous antenna elements in a device to achieve directionality. We use a cone plus circular model [13] to define the antenna gains due to main (g_m) and side (g_s) lobes of the transmitter and receiver in a two-dimensional scenario as follows:

$$g_m = \frac{2\pi}{\theta}\eta \tag{1}$$

$$g_s = \frac{2\pi}{2\pi - \theta}(1-\eta) \tag{2}$$

where, η is the antenna efficiency and θ is the beamwidth. We assume that both MiBS and FBS have the same beamwidth (i.e. $\theta' = \theta$).

The transmit pattern of a directional antenna comprises of a main lobe and a set of side lobes. The main lobe contains the maximum transmit power whereas side lobes are smaller beams that contain the remaining energy and are drawn in all directions except that of the main lobe. We assume gain because of side lobe of the MiBS antennas to be zero.

B. Channel Model

Obstacles commonly causing non Line-of-Sight (NLOS) conditions in mmWave communication include buildings, trees, hills, mountains, and, in some cases, high voltage electric power lines. We consider micro-urban Close-In (CI) path loss model [14] for LOS and NLOS, which offers substantial simplicity and more stable behavior across frequencies and distance. The path loss in CI model is calculated as follows:

$$PL(f,d) = K^{-1}d^n \tag{3}$$

$$K^{-1} = \left(\frac{4\pi f}{c}\right)^2 10^{(X_\sigma/10)} \tag{4}$$

where, $PL(f,d)$ denotes the path loss over frequency f at distance d from the transmitter, n denotes the single model parameter, c is the speed of light, and X_σ is the standard deviation describing large-scale signal fluctuations about the mean path loss over distance. We consider the effect of both LOS and NLOS to calculate the average path loss as follows:

$$PL = \alpha.PL_{LOS} + (1-\alpha).PL_{NLOS} \tag{5}$$

where, PL_{LOS} and PL_{NLOS} are the path losses in scalar due to LOS and NLOS transmission between the transmitter and the receiver. α represents the probability that a link suffers LOS losses.

C. Bitrate and SINR

We assume that the Channel Quality Information (CQI) and Signal to Interference plus Noise Ratio (SINR) are known to the MiBS at every instant of time. The SINR of an FBS in F2F link j and the SINR of the MiBS in F2M link c during uplink transmission are respectively calculated as follows:

$$\Gamma_j = \frac{KP_j^t g_j^t g_j^r d_j^{-n}}{\sum\limits_{i\in\mathcal{A},\ i\neq j} I_{j,i}^F x_i^\tau + \sum\limits_{i\in\mathcal{B}} I_{j,i}^C x_i^\tau + \sigma^2 W} \tag{6}$$

$$\text{and} \quad \Gamma_c = \frac{KP_c^t g_c^t g_c^r d_c^{-n}}{\sum\limits_{i\in\mathcal{A}} I_{c,i}^F x_i^\tau + \sum\limits_{i\in\mathcal{B},\ i\neq c} I_{c,i}^C x_i^\tau + \sigma^2 W} \tag{7}$$

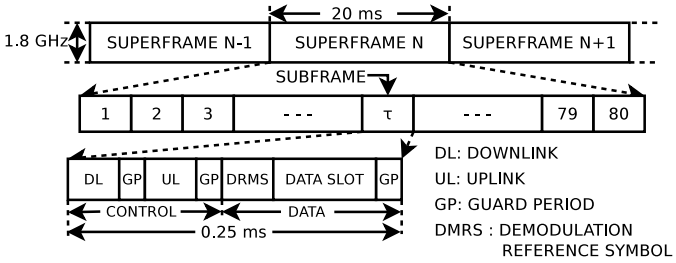

Fig. 1. 5G Small Cell Optimized Frame Format

$\mathcal{A}$ and $\mathcal{B}$ represent the set of F2F and F2M links, respectively. P_j^t (P_c^t) and g_j^t (g_c^t), are the transmit power and antenna gain of the FBS transmitter in the F2F (F2M) link. d_j (d_c) is distance between the transmitter and receiver pair in the F2F (F2M) link. Similarly, g_j^r (g_c^r) is the antenna gain of the receiver in F2F (F2M) link. $I_{j,i}^F$ and $I_{j,i}^C$ represent the interference because of F2F links and F2M links, respectively, on link j due to link i which are scheduled in the same data slot (τ). σ^2 is the Additive White Gaussian Noise. W is the channel bandwidth. x_i^τ is defined as

$$x_i^\tau = \begin{cases} 1 & \text{if link } i \in \{\mathcal{A} \cup \mathcal{B}\} \text{ is scheduled} \\ & \text{in data slot } \tau \\ 0 & \text{otherwise} \end{cases} \tag{8}$$

D. 5G Frame Format

We consider TDD based 5G small cell optimized frame format (Figure 1) proposed in [15]. In our system, MiBS controls the uplink and downlink transmissions of the FBSs in the network by suitably assigning the resources to the FBSs. MiBS broadcasts the beacons in all the directions by activating its beams in all the sectors for synchronization. As shown in Figure 1, each 20 ms superframe is divided into 80 subframes of 0.25 ms duration which consists of control and data period. An FBS and the MiBS exchange data transmission requests, location information, transmission power, and boresight direction during the control period. Moreover, the MiBS also determines the optimal transmit power of the FBSs during scheduling and communicates the same to the FBSs during the control period.

III. Problem Formulation

A. Optimization Problem

Our problem focuses on maximizing the number of links that can be scheduled concurrently in a data slot τ. We model the link requests that need to be scheduled in one superframe as a graph $G = (V, E)$, where $V = \{\mathcal{A} \cup \mathcal{B}\}$ is the set of F2F and F2M link requests sent to the MiBS for data transmission and E is the set of edges between the link requests V (as shown in Figure 4). If $(i, j) \in E$ then the transmissions due to links i and j interfere with each other (refer Section IV-B).

$$a_{ij} = \begin{cases} 1 & if\ (i,j) \in E \ \ i,j \in V \\ 0 & otherwise \end{cases} \tag{9}$$

We define ξ_τ to represent the utilization of a single data slot τ as follows:

$$\xi_\tau = \sum_{i \in V} x_i^\tau \tag{10}$$

where, x_i^τ is defined as in Equation 8.

In order to maximize the number of links scheduled in our system, we maximize the utilization of the data slots of a superframe, which can be represented as follows:

$$\max \sum_{\tau \in T} \xi_\tau \tag{11}$$

$$\text{such that,} \quad a_{ij} x_i^\tau x_j^\tau = 0 \quad \forall i, \forall j; j \neq i, \forall \tau \tag{12}$$

where, $|T|$ is the number of data slots (subframes) available in one superframe. Equation 12 represents that two interfering links i and j can not be scheduled concurrently in the same data slot τ. The optimization problem can be mapped to finding a maximal independent set problem which is a well known NP-hard problem. The search space is $O(2^{|\mathcal{A}|+|\mathcal{B}|})$ if MiBS uses exhaustive searching for scheduling the backhaul links. We propose a polynomial time heuristic scheduling algorithm by considering the unique features of mmWave networks as mentioned in Section II.

IV. Proposed Solution

In order to solve the above mmWave link scheduling problem (Eq. 11), we use greedy graph coloring algorithm on the interference matrix which is based on the interference distance between the transmitter and receiver of two neighboring links i and j, respectively. If two links are colored with same color then they can be scheduled together in the same data slot without any interference.

A. Analysing Single Transmission (Time Division Multiple Access (TDMA)) vs. Concurrent Transmissions

TDMA permits only one link to be scheduled in a particular data slot. Hence, the link does not suffer interference from any of the other links' transmission. The average data rates of link j (F2F) and link c (F2M) are respectively given by:

$$R_j = \frac{W}{|T|} \log_2(1 + \frac{K P_j^t g_j^t g_j^r d_j^{-n}}{\sigma^2 W}) \text{ and} \tag{13}$$

$$R_c = \frac{W}{|T|} \log_2(1 + \frac{K P_c^t g_c^t g_c^r d_c^{-n}}{\sigma^2 W}) \tag{14}$$

If more than one link is scheduled in a data slot (i.e., with concurrrent transmissions) a link can suffer interference from the other links. In that case using Shannon's theory [16], the average data rates of link j and link c are respectively given by:

$$R_j^{'} = W \log_2(1 + \frac{K P_j^t g_j^t g_j^r d_j^{-n}}{\sum\limits_{i \in \mathcal{A},\ i \neq j} I_{j,i}^F x_i^\tau + \sum\limits_{i \in \mathcal{B}} I_{j,i}^C x_i^\tau + \sigma^2 W}) \text{ and} \tag{15}$$

$$R_c^{'} = W\log_2(1+\frac{KP_c^t g_c^t g_c^r d_c^{-n}}{\sum\limits_{i\in\mathcal{A}} I_{c,i}^F x_i^\tau + \sum\limits_{i\in\mathcal{B},\ i\neq c} I_{c,i}^C x_i^\tau + \sigma^2 W}) \tag{16}$$

For acheiving $R_j^{'} \geq R_j$ and $R_c^{'} \geq R_c$ we need to consider two different cases:

Case 1: If $\Gamma_j < 1$ and $\Gamma_c < 1$, then the average achieved data rates $R_j^{'}$ and $R_c^{'}$ can be respectively approximated as

$$Wlog_2(1+\Gamma_j) \approx W\Gamma_j log_2 e \text{ and} \tag{17}$$

$$Wlog_2(1+\Gamma_c) \approx W\Gamma_c log_2 e \tag{18}$$

using Taylor's series expansion of $\log_e(1+\Gamma_\zeta)$ and by ignoring higher terms. $\log_e(1+\Gamma_\zeta)$ expansion is given by:

$$\log_e(1+\Gamma_\zeta) = \Gamma_\zeta - \frac{\Gamma_\zeta^2}{2} + \frac{\Gamma_\zeta^3}{3} - \frac{\Gamma_\zeta^4}{4}..., \text{ where, } \zeta \in \{j,c\} \tag{19}$$

For $\Gamma_\zeta < 1$ the expansion can be approximated to Γ_ζ. Hence $\log_2(1+\Gamma_\zeta) \approx \Gamma_\zeta / \log_e 2$. Using approximations, from Equations 13, 14, and Equations 15, 16 we obtain a sufficient condition to achieve $R_j^{'} \geq R_j$ and $R_c^{'} \geq R_c$ which is given by $I_{j,i}^F \leq \sigma^2 W$ and $I_{j,i}^C \leq \sigma^2 W$, $\forall j \neq i$. The necessary and sufficient conditions to achieve $R_j^{'} \geq R_j$ and $R_j^{'} \geq R_j$ is given by $\sum\limits_{i\in\mathcal{A},\ i\neq j} I_{j,i}^F x_i^\tau + \sum\limits_{i\in\mathcal{B}} I_{j,i}^C x_i^\tau \leq (|T|-1)\sigma^2 W$ and $\sum\limits_{i\in\mathcal{A}} I_{c,i}^F x_i^\tau + \sum\limits_{i\in\mathcal{B},\ i\neq c} I_{c,i}^C x_i^\tau \leq (|T|-1)\sigma^2 W$, respectively. The sufficient conditions look more conservative but provide a simple and practical solution from the perspective of designing a scheduling algorithm.

Case 2: If $\Gamma_j \geq 1$ and $\Gamma_c \geq 1$ the approximations in Equations 17 and 18 will not hold true. Hence, to achieve $R_j^{'} \geq R_j$ and $R_c^{'} \geq R_c$, $\log_2(1+SNR_j)/|T| \leq \log_2(1+\Gamma_j)$ and $\log_2(1+SNR_c)/|T| \leq \log_2(1+\Gamma_c)$ should hold true, respectively, which can be rewritten as $1+SNR \leq (1+\Gamma)^{|T|}$ where,

$$(1+\Gamma_\zeta)^{|T|} = 1 + |T|\Gamma_\zeta + (|T|(|T|-1)/2)\Gamma_\zeta^2 + ... \tag{20}$$

If the necessary and sufficient conditions discussed in Case 1 hold true then the derived sufficient conditions will still be valid. SNR_j (SNR_c) is the Signal to Noise Ratio of link j (c).

Hence, from Case 1 and Case 2 we can conclude that if we allow links, whose mutual interference is less than the background noise, to transmit concurrently, the average data rate acheived for each link can be higher than the TDMA scheduling. Using this we have derived the interference distance constraints based on different lobe alignments (next subsection).

B. Interference Distance Constraints

There are typically three different categories of interference possible between different types of links in an uplink transmission,

Category 1) An F2F link interferes with another F2F link.

Category 2) An F2M link interferes with an F2F link.

Category 3) An F2M link interferes with another F2M link.

Two links i ($\in V$) and j ($\in V$) can be scheduled concurrently if the interference experienced at the receiver of link i (j) from the transmitter of link j (i) is less than or equal to the background noise. There are four different threshold interference distance constraints for two neighboring links depending upon the four different lobe alignments of the directional antennas of the receiver and interfering transmitter. The four possible lobe alignments are main-main, main-side, side-main, and side-side. The interfering distances are derived based on the different gains of the main and side lobes of transmitter and receiver.

1) Constraint 1: Main Lobe-Main Lobe Alignment: The main lobe of interfering transmitter Tx_i and main lobe of interfered receiver Rx_j are aligned with each other (Figure 2), i.e. the interfering transmitter is in beamwidth of interfered receiver ($\Delta_i \leq \theta/2$) and the interfered receiver is in beamwidth of interfering transmitter ($\Delta_j \leq \theta/2$). However, Tx_i will not interfere with Rx_j if $d \geq d_{mm}$, where d is the distance between Tx_i and Rx_j.

$$d_{mm} = \left(\frac{Kg_m^t g_m^r P_t}{\sigma^2 W}\right)^{1/n} \tag{21}$$

is the maximum interference range of Tx_i when main lobe of Tx_i is aligned with main lobe of Rx_j. It is the most desirable alignment for data transfer and we assume that the main lobes of the transmitter and receiver of a link i are aligned before data transfer in order to maximize the data transfer rate.

2) Constraint 2: Main Lobe-Side Lobe Alignment: If $\Delta_i \leq \theta/2$ and $\Delta_j \geq \theta/2$ then the main lobe of interfering transmitter Tx_i and side lobe of interfered receiver Rx_j is aligned with each other i.e., the case when Rx_j is within the beamwidth of Tx_i but Tx_i is outside the beamwidth of Rx_j. However, Rx_j will not get interfered by Tx_i if $d \geq d_{ms}$, where,

$$d_{ms} = \left(\frac{Kg_m^t g_s^r P_t}{\sigma^2 W}\right)^{1/n} \tag{22}$$

3) Constraint 3: Side Lobe-Main Lobe Alignment: If $\Delta_i \geq \theta/2$ and $\Delta_j \leq \theta/2$ then side lobe of interfering transmitter Tx_i and main lobe of interfered receiver Rx_j are aligned with each other i.e., the case when Rx_j is outside the beamwidth of Tx_i but Tx_i is within the beamwidth of Rx_j. However, Rx_j will not get interfered by Tx_i if $d \geq d_{sm}$, where,

$$d_{sm} = \left(\frac{Kg_s^t g_m^r P_t}{\sigma^2 W}\right)^{1/n} \tag{23}$$

4) Constraint 4: Side Lobe-Side Lobe Alignment: If $\Delta_i \geq \theta/2$ and $\Delta_j \geq \theta/2$ then side lobe of interfering transmitter Tx_i and side lobe of interfered receiver Rx_j is aligned i.e., the case when Rx_j is outside the beamwidth of Tx_i and vice versa. However, Rx_j will not get interfered by Tx_i if $d \geq d_{ss}$, where,

$$d_{ss} = \left(\frac{Kg_s^t g_s^r P_t}{\sigma^2 W}\right)^{1/n} \tag{24}$$

MiBS and FBSs use the maximum transmission power to compute the interfering distance as described above. MiBS

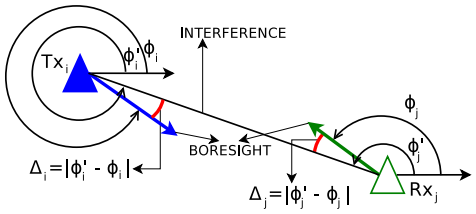

Fig. 2. Lobe Alignment

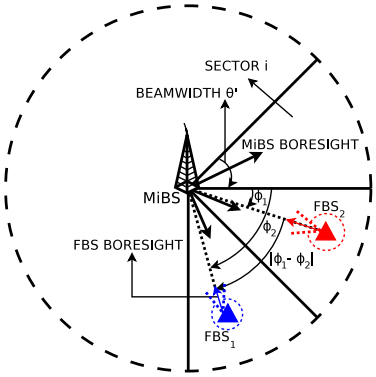

Fig. 3. Concurrent Uplink Transmission from Two FBSs

uses Constraint 1 to Constraint 4 for the Categories 1 and 2. However, for Category 3 two F2M links are considered to be non-interfering for uplink transmission if $|\phi_1 - \phi_2| > \theta'$ as shown in Figure 3.

C. Interference Matrix

The interference matrix is derived based on the interference distance as presented in the previous subsection. We construct an interference matrix of size $|V| \times |V|$, where $|V|$ is the total number of link requests including both F2F and F2M links. a_{ij} represents the interference between the links i and j at j^{th} column of i^{th} row of the interference matrix. If the links i and j cannot be scheduled together due to high interference then the value of j^{th} column of i^{th} row of the interference matrix is 1, 0 otherwise. Algorithm 1 presents the procedure with $O(V^2)$ time complexity for determining the interference matrix by using the constraints derived in the previous subsection.

D. Concurrent Link Scheduling with Power Control (CLSPC)

In this section, we propose a heuristic based polynomial time scheduling algorithm for the optimization problem discussed in Section III. For scheduling decision we have ignored the mobility of FBS because the position of FBS is fixed at the roof top (as stated in Section II). Thus, the received signal power and interference power at the receiving base station (FBS or MiBS) will not change significantly. We have assumed that the MiBS has a global knowledge of the network topology, for example, location of the FBS, number of active links (F2F or F2M) etc.

Once the interference graph G obtained from the interference matrix is colored with the greedy graph coloring of time complexity $O(V^2 + E)$, all the non-interfering links colored with the same color can be scheduled concurrently in the same data slot. Given a set of colors, greedy coloring algorithm never uses more than $\Psi + 1$ colors, where Ψ is the degree of the vertex. The greedy algorithm colors first (any) vertex with the first color. For the remaining $V-1$ vertices it considers the currently picked vertex and colors it with a color that has not been used on any previously colored vertices adjacent to it. If all previously used colors appear on vertices adjacent to v, it assigns a new color to it. The number of colors determines the number of data slots required to schedule all the links. Initially all the FBSs transmit with the maximum transmit power P_{max}. However, as the mmWave links have high directional gain antennas, link SINR can be sufficiently high (i.e. achieved data rate can be higher than the required QoS). In such a situation, the transmit power of the transmitter can be reduced while maintaining the requested QoS. Performing power control reduces the interference among the different links which otherwise interfere with each other in the maximum transmit power mode.

Algorithm 1 Interference Matrix Determination

```
1: procedure FINDINTERFERENCEMATRIX(V)
2:     for each i ∈ V do
3:         for each j ∈ V − i do
4:             d ← getDistance(Tx_i, Rx_j)
5:             if (i ∈ A & j ∈ A) or (i ∈ A & j ∈ B)
                or (i ∈ B & j ∈ A) then
6:                 if ∠Δ_i ≤ θ/2 & ∠Δ_j ≤ θ/2 &
                    d ≤ d_mm then
7:                     IM(i, j) ← 1
8:                 else if ∠Δ_i ≤ θ/2 & ∠Δ_j ≥ θ/2 &
                    d ≤ d_ms then
9:                     IM(i, j) ← 1
10:                else if ∠Δ_i ≥ θ/2 & ∠Δ_j ≤ θ/2 &
                    d ≤ d_sm then
11:                    IM(i, j) ← 1
12:                else if ∠Δ_i ≥ θ/2 & ∠Δ_j ≥ θ/2 &
                    d ≤ d_ss then
13:                    IM(i, j) ← 1
14:                else
15:                    IM(i, j) ← 0
16:                end if
17:            else if (i ∈ B & j ∈ B) then
18:                if |φ_1 − φ_2| > θ' then
19:                    IM(i, j) ← 0
20:                else
21:                    IM(i, j) ← 1
22:                end if
23:            end if
24:        end for
25:    end for
26: end procedure
```

The CLSPC determines the transmit power with which an FBS should transmit to maintain the required QoS based on the channel conditions. The receiver MiBS or FBS instructs the transmitter FBS to reduce its transmission power such that the QoS is satisfied. The reduced transmission power of an FBS transmitter of link i can be determined by the MiBS as follows:

$$P_t^i = min\left(\frac{(2^{Q_i/W} - 1)(I + \sigma^2 W)}{g_m^t g_m^r K d^{-n}}, P_{max}\right) \quad (25)$$

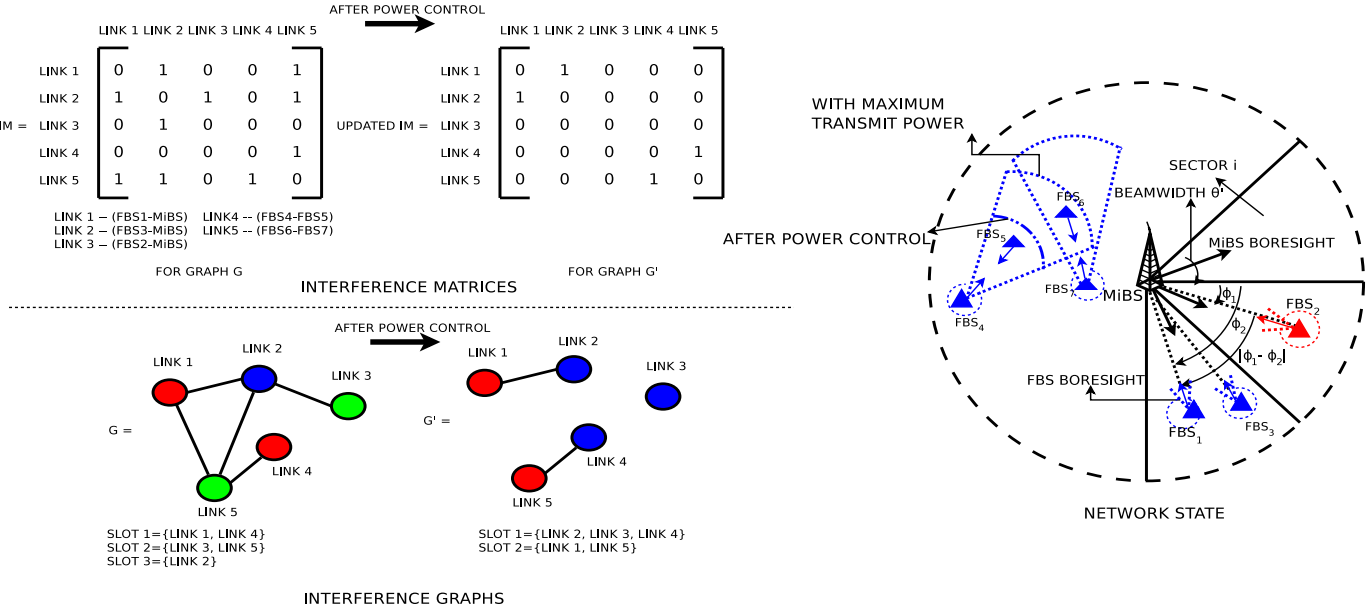

Fig. 4. Interference Matrix (IM), Interference Graph, and Network Scenario

Algorithm 2 Concurrent Link Scheduling with Power Control

procedure CLSPC(V)
  $IM \leftarrow FindInterferenceMatrix(V)$
  repeat
    $concLinkSubsets \leftarrow graphColoring(IM)$
    for each $concLinks \in concLinkSubsets$ **do**
      for each $link \in concLinks$ **do**
        $Q_i \leftarrow getQoSDemand(link)$
        $t \leftarrow getTransmitter(link)$
        $r \leftarrow getReceiver(link)$
        $I \leftarrow getInterferenceAtReceiver(r)$
        $d \leftarrow getDistance(t, r)$
        if $\frac{(2^{\frac{Q_i}{W}}-1)(I+\sigma^2 W)}{g_m^t g_m^r K d^{-n}} < P_{max}$ **then**
          $setTxPower(t, \frac{(2^{\frac{Q_i}{W}}-1)(I+\sigma^2 W)}{g_m^t g_m^r K d^{-n}})$
        else
          $setTxPower(t, P_{max})$
        end if
      end for
    end for
    update IM based on power control
  until $InterferenceMatrix$ *converges*
  $concLinkSubsets \leftarrow graphColoring(IM)$
  for each $concLinks \in concLinkSubsets$ **do**
    $scheduleConcurrently(slot, concLinks)$
    $slot \leftarrow slot + 1$
  end for
end procedure

where, Q_i and I are the QoS requirement and interference experienced by link i, respectively. P_{max} is the maximum transmit power of an FBS.

Algorithm 2 describes the Concurrent Link Scheduling with Power Control. MiBS computes the interference matrix with the modified transmit power of the FBSs by using constraints described in Section IV-B. This process of reducing the transmit power and interference matrix computation is repeated until the new interference matrix and old interference matrix computed earlier are different. Once the interference matrix converges MiBS applies the graph coloring on the graph G obtained from latest interference matrix and schedules the links concurrently colored with the same color in the same data slot. If Algorithm 2 converges in κ steps then its time complexity is $O(\kappa V^2)$. In our model, the scheduling is performed in every superframe. All the requests that are gathered in the superframe n-1 are scheduled in superframe n. Moreover, MiBS performs the scheduling and power control whenever a new link is added or dropped, or there is a change in QoS demand of a link in the next superframe. Figure 4 shows an example of interference matrix and interference graph, and also shows the network state corresponding to the updated interference matrix and updated interference graph after performing the power control.

V. Performance Evaluation

The simulation scenario consists of a set of FBSs deployed uniformly within the coverage area of an MiBS of radius 200 meters. The MiBS is located at the center of the coverage area. All the FBSs are equipped with an electronically steerable directional antenna. The MiBS is equipped with multiple directional antennas with a fixed boresight beamforming to its corresponding sectors as shown in Figure 3. The number of FBS data transmission requests is varied from 10 to 100 that consists of both F2M and F2F communication requests. The QoS demand of each backhaul link is taken uniformly between 3.56 Gbps and 7.12 Gbps. Each data point is averaged over the results of 1000 different simulation instances and the results are presented with 95% confidence interval. We have considered a TDD based 5G frame structure as proposed in [15] with a single subcarrier of bandwidth 1.8 GHz in our simulation. All the simulation parameters for the mmWave system are shown in Table I.

Our work is first of its kind and therefore it cannot be

TABLE I
SIMULATION PARAMETERS

Parameter	Value
MiBS Coverage (R)	200 meters
Number of FBSs (F)	20-200
Uplink Bandwidth (W)	1.8 GHz
Carrier Frequency(f)	60 GHz
MiBS Transmit Power	30 dBm
FBS Transmit Power (P_{max})	23 dBm
Single Model Parameter (n) for LOS, NLOS	2.0, 3.1
Standard Deviation (X_σ) for LOS, NLOS	2.9 dB, 8.1 dB
Additive White Gaussian Noise (AWGN) (σ^2)	-134 dBm/MHz

compared with prior work in the literature due to the differences in the system model and the use of F2F communication. Therefore, we have compared our proposed scheme CLSPC with the naive TDMA based link scheduling and random link scheduling. In TDMA approach only one link is scheduled in a particular data slot whereas in random scheme links are taken randomly to be scheduled in a particular data slot. For a fair comparison, all the schemes use F2F communication.

To analyze the performance of all the schemes, we plot uplink system throughput while varying number of link requests, antenna efficiency and beamwidth; and number of concurrent transmissions while varying beamwidth (θ).

In Figure 5 ($\eta = 0.8,\ \alpha = 0.8,\ \theta = 40°$), we examine the performance of uplink throughput by varying number of link requests. On varying the number of link requests, the uplink throughput remains almost same for TDMA as at most one link is scheduled in a data slot (subframe). The random scheduling achieves throughput higher than that of TDMA based scheduling because multiple links are scheduled concurrently in one data slot. However, the links scheduled randomly may cause very high interference with each other. Our proposed CLSPC scheme schedules multiple non-interfering links in one data slot which achieves throughput higher than that of random scheduling. Also, our proposed CLSPC scheme controls the transmit power of an FBS while satisfying the QoS requirement of links. This further reduces the interference among the links. Hence, a larger number of links are scheduled concurrently.

In Figure 6 ($\eta = 0.8,\ \alpha = 0.8,\ \theta = 40°$), we analyze the number of concurrent transmissions possible by varying the number of link requests. For all the values of the number of links requests, our proposed scheme CLSPC always outperforms the other two candidate schemes i.e., TDMA and random scheduling. This is because the proposed scheme utilizes the data slot more efficiently by scheduling the non-interfering links while exploiting direct F2F communication.

It should be noted that the average data rate of each link will decrease when there are more active backhaul links in the network due to the increased interference. However, because of the more concurrent transmissions as shown in Figure 6, uplink throughput will be increased.

We investigate the average uplink throughput versus antenna efficiency in Figure 7 ($Number\ of\ links = 40,\ \alpha = 0.8,\ \theta = 40°$). It can be noted that for all the schemes uplink throughput increases on increasing the antenna efficiency (η) because of

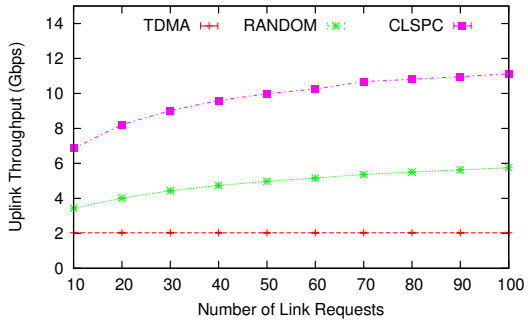

Fig. 5. Uplink Throughput vs. Number of Link Requests

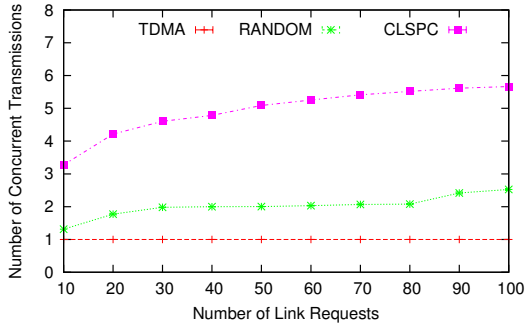

Fig. 6. Number of Concurrent Transmissions vs. Number of Link Requests

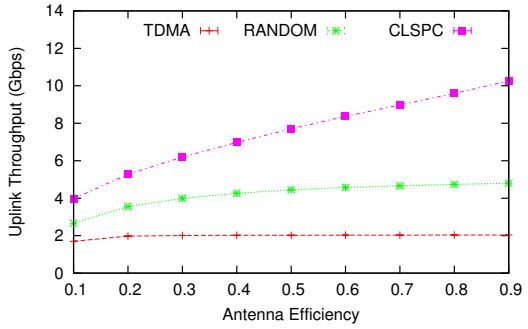

Fig. 7. Uplink Throughput vs. Antenna Efficiency

increase in the gain in the main lobe and decrease in the gain in the side lobe which further increases the received signal strength of the intended receiver and increases the SINR of the link. Our proposed scheme attains higher throughput as compared to TDMA and random scheduling because it concurrently schedules non-interfering links.

Figure 8 ($Number\ of\ links = 40,\ \alpha = 0.8,\ \eta = 0.8$), depicts the performance of uplink throughput for 3 different values of beamwidth. From the figure, it can be concluded that for all the schemes uplink throughput decreases on increasing the beamwidth because on increasing the beamwidth, the transmitted signal can cover larger area. This will cause more interference to the other links and reduces the number of concurrent transmissions. However, our proposed scheme beats the other two schemes because of increase in spatial reuse on decreasing the beamwidth and scheduling the links concurrently which are non-interfering. This helps in increasing the number of concurrent link transmissions which reduces the number of data slots (subframes) required to schedule the

links and increases the uplink throughput.

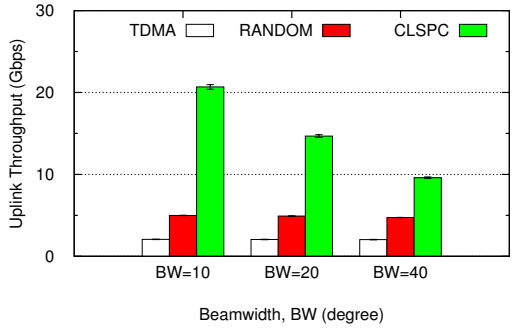

Fig. 8. Uplink Throughput vs. Beamwidth (BW)

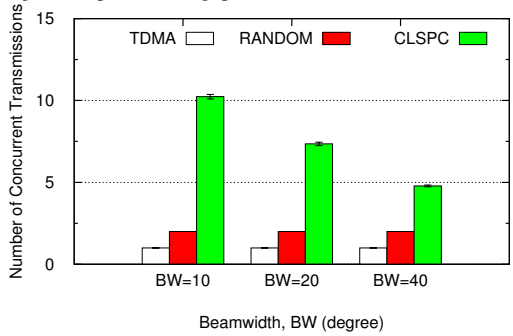

Fig. 9. Number of Concurrent Transmissions vs. Beamwidth (BW)

In Figure 9 ($Number\ of\ links = 40,\ \alpha = 0.8,\ \eta = 0.8$), we study the performance of number of concurrent transmissions for the 3 different values of beamwidth. Our proposed scheme CLSPC outperforms the other schemes for all the values of beamwidth. This is due to appropriately selecting the non-interfering links and scheduling them concurrently in the same slot. The reason for the more number of concurrent transmissions at a lower value of beamwidth as compared to higher value is that higher value of beamwidth covers a larger area and hence, decreases the spatial reuse.

VI. Conclusion

In contrast to the existing research on mmWave transmission and link scheduling which mostly concentrated on WLAN and WPAN, in this paper we focused on backhaul link scheduling for mmWave cellular systems. To achieve high resource utilization in mmWave based 5G cellular networks we proposed direct F2F communication which not only helps in offloading the data traffic from MiBS when the user traffic is destined to the same cell but also can act as a relay link for the other FBSs for routing the backhaul traffic to MiBS. We also proposed an efficient concurrent backhaul link scheduling scheme that exploits spatial reuse by using directional antennas. To increase the number of concurrent links scheduled in a data slot we control transmit power of a link while satisfying the required QoS demand. We also studied the impact on the uplink throughput and on number of concurrent transmissions by varying number of backhaul link requests, beamwidth, and antenna efficiency for different scheduling schemes. Through extensive simulations, we demonstrated the superiority of our proposed backhaul link scheduling scheme over TDMA and random backhaul link scheduling schemes. Our work considered F2M and F2F links independently without considering the routing decision involved. Future extensions of this work can analyze uplink transmissions by considering routing decisions and can investigate the results analytically.

Acknowledgement

Thanks are due to Dr. Sudeepta Mishra for his comments and suggestions on an earlier draft of this paper, and valuable discussions. This research work was supported by the Department of Science and Technology (DST), New Delhi, India.

References

[1] D. Choudhury, "5G wireless and millimeter wave technology evolution: An overview," in *Proceedings of the IEEE MTT-S International Microwave Symposium*, 2015, pp. 1–4.

[2] V. Chandrasekhar, J. G. Andrews, and A. Gatherer, "Femtocell networks: A survey," *IEEE Communications Magazine*, vol. 46, no. 9, pp. 59–67, 2008.

[3] I. Hwang, B. Song, and S. Soliman, "A holistic view on hyper-dense heterogeneous and small cell networks," *IEEE Communications Magazine*, vol. 51, no. 6, pp. 20–27, June 2013.

[4] Y. Niu, Y. Li, D. Jin, L. Su, and A. V. Vasilakos, "A survey of millimeter wave communications (mmwave) for 5G: Opportunities and challenges," *Wireless Networks*, vol. 21, no. 8, pp. 2657–2676, 2015.

[5] S. Rangan, T. S. Rappaport, and E. Erkip, "Millimeter-wave cellular wireless networks: Potentials and challenges," *Proceedings of the IEEE*, vol. 102, no. 3, pp. 366–385, 2014.

[6] Z. Pi and F. Khan, "An introduction to millimeter-wave mobile broadband systems," *IEEE Communications Magazine*, vol. 49, no. 6, pp. 101–107, 2011.

[7] P. Pietraski, D. Britz, A. Roy, R. Pragada, and G. Charlton, "Millimeter wave and terahertz communications: Feasibility and challenges," *ZTE Communications*, vol. 10, no. 4, 2012.

[8] L. X. Cai, L. Cai, X. Shen, and J. W. Mark, "Rex: A randomized EXclusive region based scheduling scheme for mmwave WPANs with directional antenna," *IEEE Transactions on Wireless Communications*, vol. 9, no. 1, pp. 113–121, January 2010.

[9] W. ur Rehman, J. Han, C. Yang, M. Ahmed, and X. Tao, "On scheduling algorithm for Device-to-Device communication in 60 GHz networks," in *Proceedings of the IEEE Wireless Communications and Networking Conference (WCNC)*, April 2014, pp. 2474–2479.

[10] J. Qiao, L. X. Cai, X. Shen, and J. W. Mark, "STDMA-based scheduling algorithm for concurrent transmissions in directional millimeter wave networks," in *Proceedings of the IEEE International Conference on Communications (ICC)*, June 2012, pp. 5221–5225.

[11] J. Qiao, X. S. Shen, J. W. Mark, Q. Shen, Y. He, and L. Lei, "Enabling Device-to-Device communications in millimeter-wave 5G cellular networks," *IEEE Communications Magazine*, vol. 53, no. 1, pp. 209–215, January 2015.

[12] Y. M. Tsang, A. S. Poon, and S. Addepalli, "Coding the beams: Improving beamforming training in mmwave communication system," in *Proceedings of the IEEE Global Telecommunications Conference (GLOBECOM)*, 2011, pp. 1–6.

[13] R. Ramanathan, "On the performance of ad hoc networks with beamforming antennas," in *Proceedings of the ACM International Symposium on Mobile Ad Hoc Networking & Computing (MobiHoc)*, October 2001, pp. 95–105.

[14] S. Sun, T. S. Rappaport, S. Rangan, T. A. Thomas, A. Ghosh, I. Z. Kovacs, I. Rodriguez, O. Koymen, A. Partyka, and J. Jarvelainen, "Propagation path loss models for 5G urban micro- and macro-cellular scenarios," in *Proceedings of the IEEE Vehicular Technology Conference (VTC Spring)*, May 2016, pp. 1–6.

[15] P. Mogensen, K. Pajukoski, E. Tiirola, E. Lhetkangas, J. Vihril, S. Vesterinen, M. Laitila, G. Berardinelli, G. W. O. D. Costa, L. G. U. Garcia, F. M. L. Tavares, and A. F. Cattoni, "5G small cell optimized radio design," in *Proceedings of the IEEE GlOBECOM Workshops (GC Wkshps)*, December 2013, pp. 111–116.

[16] C. E. Shannon, "A mathematical theory of communication," *ACM SIGMOBILE Mobile Computing and Communications Review*, vol. 5, no. 1, pp. 3–55, 2001.